Cell

The Fragile X Syndrome Protein Represses Activity-Dependent Translation through CYFIP1, a New 4E-BP

Ilaria Napoli,[1,2,3] Valentina Mercaldo,[2,3] Pietro Pilo Boyl,[3] Boris Eleuteri,[2] Francesca Zalfa,[2,4] Silvia De Rubeis,[1,3] Daniele Di Marino,[1] Evita Mohr,[5] Marzia Massimi,[6] Mattia Falconi,[1] Walter Witke,[6] Mauro Costa-Mattioli,[7] Nahum Sonenberg,[7] Tilmann Achsel,[2,3] and Claudia Bagni[2,3,4,*]

[1]Department of Biology, University "Tor Vergata," 00133 Rome, Italy
[2]Department of Experimental Neuroscience, Fondazione Santa Lucia, IRCCS, 00143 Rome, Italy
[3]Department of Molecular and Developmental Genetics/VIB11, Catholic University of Leuven, B-3000 Leuven, Belgium
[4]Department of Experimental Medicine and Biochemical Sciences, University "Tor Vergata," 00133 Rome, Italy
[5]Department of Anatomy I- Cellular Neurobiology, University Hospital Hamburg-Eppendorf, D-20246 Hamburg, Germany
[6]European Molecular Biology Laboratory, Mouse Biology Unit, 00016 Rome, Italy
[7]Department of Biochemistry, McGill University, Montreal QC H3G 1V6, Canada
*Correspondence: claudia.bagni@med.kuleuven.be
DOI 10.1016/j.cell.2008.07.031

SUMMARY

Strong evidence indicates that regulated mRNA translation in neuronal dendrites underlies synaptic plasticity and brain development. The fragile X mental retardation protein (FMRP) is involved in this process; here, we show that it acts by inhibiting translation initiation. A binding partner of FMRP, CYFIP1/Sra1, directly binds the translation initiation factor eIF4E through a domain that is structurally related to those present in 4E-BP translational inhibitors. Brain cytoplasmic RNA 1 (*BC1*), another FMRP binding partner, increases the affinity of FMRP for the CYFIP1-eIF4E complex in the brain. Levels of proteins encoded by known FMRP target mRNAs are increased upon reduction of CYFIP1 in neurons. Translational repression is regulated in an activity-dependent manner because BDNF or DHPG stimulation of neurons causes CYFIP1 to dissociate from eIF4E at synapses, thereby resulting in protein synthesis. Thus, the translational repression activity of FMRP in the brain is mediated, at least in part, by CYFIP1.

INTRODUCTION

The construction of neuronal circuits in the developing brain requires the correct assembly of trillions of synaptic connections. Finely regulated protein synthesis may be required to obtain the correct set of proteins at synapses and to modulate their activity in response to different developmental cues or synaptic stimulations. Indeed, accumulating evidence indicates that local (synaptodendritic) protein synthesis modulates synaptic plasticity (Martin et al., 2000; Steward and Schuman, 2003; Pfeiffer and Huber, 2006; Lin and Holt, 2008). Although the general translational machinery has been found at or near synapses, components that might control specific mRNA translation in that compartment are largely unknown.

One protein implicated in neuronal mRNA translation is the fragile X mental retardation protein (FMRP), the absence of which causes the fragile X syndrome (FXS) that is characterized at the cellular level by a deficit in synapse maturation. FMRP is an RNA-binding protein with roles in mRNA localization, translation (Bagni and Greenough, 2005), and stability (Zalfa et al., 2007; Zhang et al., 2007). It recognizes mRNAs by directly interacting with them through G quartets and/or U-rich sequences or through small, noncoding RNA adaptors such as the brain cytoplasmic RNA *BC1* and possibly microRNAs (Bagni and Greenough, 2005). Strong evidence indicates that FMRP represses translation, although how it does so is enigmatic.

Two well-characterized pathways that affect local protein synthesis in neurons involve activation of the TrkB receptors (Steward and Schuman, 2003; Schratt et al., 2004) by the neurotrophin BDNF and stimulation of the group 1 metabotropic glutamate receptors (mGluRs) (Weiler and Greenough, 1993). BDNF treatment activates the translation of two dendritic FMRP target mRNAs that encode Arc/Arg3.1 and αCaMKII (Aakalu et al., 2001; Yin et al., 2002; Zalfa et al., 2003; Schratt et al., 2004). On the other hand, FMRP is also regulated in response to mGluR stimulation (Weiler et al., 1997; Antar et al., 2004; Ferrari et al., 2007); moreover, long-term depression (LTD), triggered by activation the of mGluRs, is enhanced in the hippocampus of mutant mice lacking FMRP (Huber et al., 2002).

One possible mechanism for regulating translation is by modulation of the interactions between factors required for translational initiation. Cap-dependent translation, which requires the association of the eIF4A-eIF4G-eIF4E (eIF4F) complex with the 5′ terminal m^7G cap, is known to be particularly important in neurons (Richter and Sonenberg, 2005). eIF4F assembly is often regulated by the 4E binding proteins (4E-BPs), which interfere with the eIF4E-eIFG interaction (Richter and Sonenberg, 2005; Richter and Klann, 2007; Banko et al., 2007). eIF4E-binding proteins, including 4E-T and eIF4G, share a motif that is responsible

for their association with eIF4E. Although 4E-BP1, BP2, BP3, and 4E-T, which all block the eIF4G-eIF4E interaction, probably act as general regulators, other proteins such as *Xenopus* Maskin and *Drosophila* Cup act as mRNA-specific 4E-BPs (Richter and Sonenberg, 2005). Thus far, only Neuroguidin has been identified as a 4E-BP in the nervous system (Jung et al., 2006).

Here, we demonstrate that FMRP-mediated repression of translation requires an interaction with *Cy*toplasmic *F*MRP *I*nteracting *P*rotein CYFIP1 (Schenck et al., 2001; Schenck et al., 2003) also known as Sra-1 (Kobayashi et al., 1998), which also binds the cap-binding factor eIF4E. The eIF4E-interacting domain of CYFIP1 forms the characteristic "reverse L shaped" structure that is also assumed by the canonical eIF4E-binding motif (Marcotrigiano et al., 1999). Modulation of CYFIP1 levels affects general mRNA translation in mammalian cells. In the brain, however, CYFIP1 forms a complex with specific FMRP-target mRNAs; reduced levels of CYFIP1 cause an increase in the synthesis of MAP1B, αCaMKII, and APP, whose mRNAs are known to be regulated by FMRP (Bagni and Greenough, 2005; Hou et al., 2006; Westmark and Malter, 2007). Our data indicate that an eIF4E-CYFIP1-FMRP complex is present at synapses and that synaptic activity releases CYFIP1 from eIF4E, as well as from bound RNAs, resulting in the alleviation of translation repression.

RESULTS

FMRP Cosediments with Light mRNPs in a Complex Possibly Containing Both eIF4E and CYFIP1

To investigate the mechanism by which FMRP represses translation in neurons, we examined the distribution of FMRP in sucrose gradients. As shown in Figure 1A, FMRP cofractionated with mRNPs with sedimentation values ranging from 40S to 80S. This profile is similar to the one observed for translational regulators such as mammalian p27/eIF6 and eIF4E (Figure 1A and Figure S1 available online). Interestingly, CYFIP1, which interacts with FMRP in the cytoplasm (Schenck et al., 2001), partially cofractionated with FMRP and eIF4E (Figure 1A, lanes 6–9, and Figure S1). Poly(A)-binding protein (PABP), which associates with translationally active and inactive mRNAs, cosedimented with mRNPs (Figure 1A), as well as with heavy polysomes (Figure S1). These sedimentation experiments suggest that FMRP, CYFIP, and eIF4E might reside in a common complex, perhaps with mRNA.

The FMRP-CYFIP1 Complex Binds eIF4E and PABP in Brain

We next investigated whether the FMRP-CYFIP1 complex could be retained with eIF4E on m^7GTP-Sepharose. When the beads were incubated with total brain cytoplasmic extracts, both FMRP and CYFIP1 were recovered from them but only after specific elution with m^7GTP (Figure 1B, lane 3). Whereas the recovery of FMRP varied according to salt concentration (data not shown), CYFIP1 recovery was not particularly salt sensitive. PABP was also present in the m^7GTP eluate, whereas two other proteins not involved in mRNA translation, β-tubulin and reticulon 1C, were not specifically eluted. Interestingly, WAVE, a cytoplasmic protein interacting with CYFIP1 (Bogdan et al., 2004), was also mostly not retained on the beads (Figure 1B, lane 3), suggesting a specific function of the FMRP-CYFIP1-eIF4E complex. Furthermore, neither CYFIP1 nor FMRP (Figure 1B, compare lanes 5 and 6) was present in the last wash; GTP greatly reduced the yield of the eluted complex (Figure 1B, lane 7), demonstrating the efficiency and specificity of the m^7GTP elution.

The FMRP-CYFIP1-eIF4E complex was also coprecipitated from brain extracts with specific FMRP antibody (Ferrari et al., 2007). A specific interaction among FMRP, eIF4E, and CYFIP1 was detected in wild-type (Figure 1C, lane 4) but not in *FMR1* knockout (KO) mice (Figure 1C, lane 3) (Bakker et al., 1994). RNase A treatment did not destroy the CYFIP1-FMRP-eIF4E interaction as assessed by CYFIP1 antibody coprecipitation (Figure 1D, compare lanes 2 and 6, and Figure S2), although a decrease in the FMRP-CYFIP1 association did occur (see below). These data indicate that the FMRP-CYFIP1-eIF4E complex is maintained primarily by protein-protein interactions.

To investigate whether the binding of the CYFIP1-FMRP complex to m^7GTP was mediated by FMRP, we performed m^7GTP chromatography with *FMR1* KO brain extracts (Figure 1E). The eIF4E-CYFIP1 association did not require FMRP (Figure 1E, lane 3). Furthermore, addition of exogenous human 4E-BP1 (Haghighat et al., 1995) to brain extracts decreased the amount of FMRP-CYFIP1 bound to eIF4E (Figure 1F, lanes 2–4), suggesting that they competed for the same site on eIF4E. This was confirmed with a 4E-BP mutated in the eIF4E-binding site (Figure S3). We conclude from these data that the FMRP-CYFIP1 complex binds eIF4E.

Translational repression occurs when 4E-BPs bind eIF4E to the exclusion of eIF4G (Marcotrigiano et al., 1999; Richter and Sonenberg, 2005). Consequently, we investigated whether the absence of a functional eIF4GI impaired the binding of CYFIP1-FMRP complex to eIF4E. After inactivation of eIF4GI by cleavage (Gradi et al., 1998) (Figure 1G, lane 1, asterisk), CYFIP1 and FMRP still bound eIF4E (Figure 1G, lane 2), indicating that binding of CYFIP1 to eIF4E does not require functional eIF4G.

PABP at the 3′ terminus of mRNA interacts with the 5′ cap-binding complex and circularizes mRNAs (Mazumder et al., 2003). Furthermore, the noncoding RNA *BC1*, which resides in the FMRP complex (Zalfa et al., 2003, 2005; Gabus et al., 2004; Johnson et al., 2006; Centonze et al., 2007b) also binds PABP (West et al., 2002). To test whether the FMRP-CYFIP1 complex simultaneously interacts with PABP, we used poly(A)-Sepharose beads to isolate PABP and associated factors from brain extracts. The FMRP-CYFIP1 complex was recovered together with PABP (Figure S4A). The binding of CYFIP1 to PABP was independent of FMRP and *BC1* RNA, as shown by the use of *FMR1* and *BC1* KO (Skryabin et al., 2003) brain extracts (Figure S4A). Moreover, the recovery of the FMRP-CYFIP1 complex was not due to nonspecific binding of CYFIP1 or FMRP to the polyribonucleotides affixed to the beads (Figure S4B). PABP and FMRP were also coimmunoprecipitated (Figure 1C, lane 4), indicating that FMRP and CYFIP1 are present in a complex containing both eIF4E and PABP.

CYFIP1 Binds Directly and Specifically to eIF4E

Because CYFIP1 bound m^7GTP (Figure 1B) independently of FMRP (Figure 1E), we hypothesized that CYFIP1 might be a novel

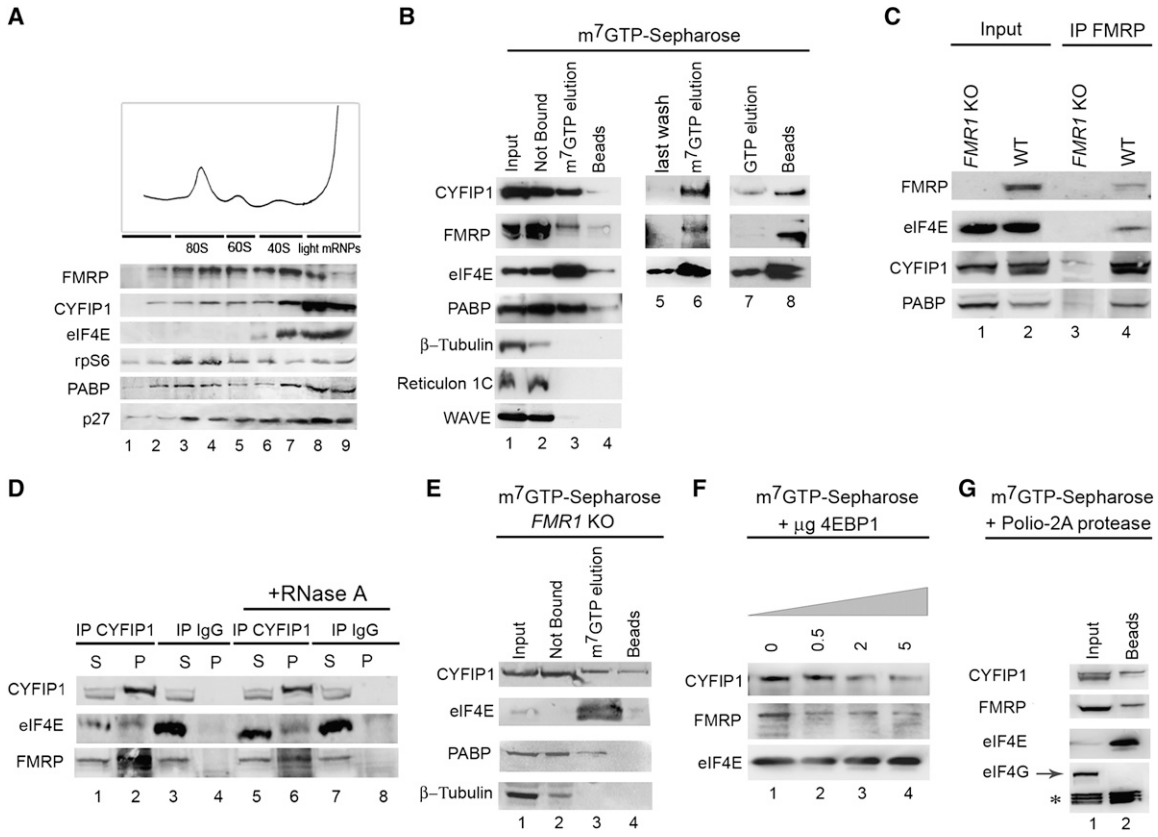

Figure 1. FMRP-CYFIP1 mRNP Interacts with the Translational Initiation Complex

(A) Cosedimentation of proteins on a 5%–25% sucrose gradient. The 80S monosome, the 60S and 40S subunits, and the very light mRNPs were detected by absorbance of 254 nm light. FMRP, CYFIP1, eIF4E, ribosomal protein S6 (rpS6), PABP, and eIF6/p27 were detected by immunoblotting.

(B) The initiation complex contains CYFIP1. Mouse brain proteins eluted from m^{7}GTP-Sepharose by free m^{7}GTP were analyzed by immunoblotting for CYFIP1, FMRP, eIF4E, PABP, β-Tubulin, Reticulon 1C, and WAVE. Lane 1, input (1/20); lane 2, unbound proteins (1/20); lane 3, specific elution with free m^{7}GTP; and lane 4, proteins retained on the beads after m^{7}GTP elution (beads). CYFIP1 and FMRP are absent from the last wash (lane 5) and in the GTP elution (lane 7). Proteins recovered after specific (lane 6) and nonspecific (lane 7) elution. Lane 8, proteins bound to the beads after nonspecific elution.

(C) CYFIP1 and eIF4E are both present in the FMRP complex in vivo. Western blot of proteins from *FMR1* KO and wild-type (WT) mouse brain extracts (Input [1/10], lanes 1 and 2, respectively) and proteins recovered after immunoprecipitation of the FMRP complex. Lane 4 shows detection of FMRP, eIF4E, CYFIP1, and PABP. Lane 3 is as above in the *FMR1* KO extracts.

(D) CYFIP1-eIF4E and CYFIP1-FMRP interactions resist RNase treatment. Lanes 2 and 6 show western blot of proteins recovered after immunoprecipitation of the CYFIP1 complex from WT mouse brain extracts. Lanes 1 and 3 show supernatants (1/20) after immunoprecipitation with CYFIP1 antibody and rabbit IgG. Lanes 5 and 7 show supernatants (1/20) after CYFIP1 and IgG immunoprecipitation in the presence of RNase. Lanes 4 and 8 show immunoprecipitations with rabbit IgG.

(E) FMRP absence does not interfere with CYFIP1-eIF4E complex formation. The same experiment as in (B) was performed with *FMR1* KO mouse brain extract. Lane 1, input (1/20); lane 2, unbound proteins; lane 3, m^{7}GTP-eluted proteins; and lane 4, proteins recovered from the beads after m^{7}GTP elution (Beads).

(F) Human 4E-BP1 competes with CYFIP1 for eIF4E binding. Lane 1, specifically eluted proteins (same as in [B]). Lanes 2–4, increasing amounts of wild-type human 4E-BP1 were added to brain extracts before m^{7}GTP chromatography (lanes 2–4). Western blotting was used to detect the levels of bound CYFIP1, FMRP and eIF4E.

(G) CYFIP1 binds the eIF4E complex independent of eIF4G. Lane 1, input (1/20) of the HeLa cytoplasmic extracts incubated with Polio-2A protease; lane 2, proteins retained on the column.

eIF4E-binding protein. eIF4G and several characterized 4E-BPs share a short consensus motif that is responsible for binding to eIF4E (Richter and Sonenberg, 2005). Therefore, we used multi-sequence alignments to search for a similar peptide that is conserved in the CYFIP protein family. A candidate peptide (residues 733 to 751, human CYFIP1, Swissprot annotation Q14467) was identified in the central region of CYFIP1. Here, several amino acids are conserved among CYFIP and human 4E-BPs, 4G-I, and 4G-III (Figure 2A). To validate the functional significance of this similarity, we compared a structural arrangement of the CYFIP1 peptide spanning residues 733 to 751 with the known structure of eIF4E when complexed with the 4E-BP1 peptide (Tomoo et al., 2005). Indeed, the CYFIP1 peptide (blue ribbon in Figure 2B) could potentially adopt the peculiar "reverse L shaped" structure with two α-helical turns located at its center that are stabilized by two internal salt bridges between residues Asp742-Arg744 and Glu748-Lys750. Moreover, the CYFIP1 peptide docks onto the molecular binding surface of eIF4E (red

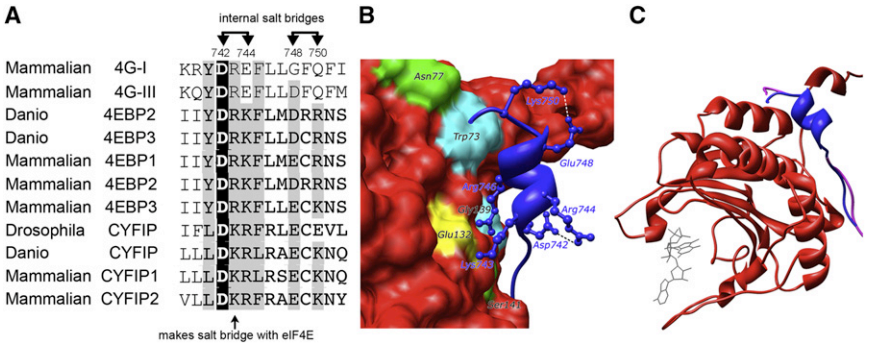

Figure 2. Multiple Alignment of Mammalian, Zebrafish, and *Drosophila* CYFIP1 and Canonical 4E-BPs

(A) The gray and black-boxed amino acids in the multiple sequence alignment are conserved and identical residues, respectively, that fold and interact with eIF4E. Black arrows denote internal salt bridges and one salt bridge with eIF4E.

(B) Hypothetical interactions between eIF4E, represented as a red molecular surface, and CYFIP1 peptide, shown as a blue spiral ribbon.

(C) Structural prediction of a complex among 4E-BP (red), the m^7GTP cap (gray molecule), and the CYFIP1 peptide (blue). The 4E-BP peptide (purple) found in the crystal structure almost perfectly overlaps with the CYFIP1 peptide.

(B) and (C) were produced with the UCSF Chimera program (Pettersen et al., 2004).

ribbon; Figures 2B and 2C), where 12 out of the 16 interactions formed between eIF4E and 4E-BP1 (Marcotrigiano et al., 1999; Tomoo et al., 2005) are conserved. In particular, the internal salt bridge Asp742-Arg744 (Figure 2B and Figure S6A) restricts the available conformations of the basic residue Lys743 and is thus locked in a favorable position for the formation of a salt bridge with Glu132 of eIF4E (Figure 2B). The 4E-BP1 peptide (purple ribbon, Figure 2C) and the CYFIP1 binding peptide (blue ribbon, Figure 2C) overlap in their "reverse L shaped" predicted structure and fit into the eIF4E pocket. The m^7GTP-Sepharose chromatography (Figure 1) and the in silico analysis (Figure 2) predict that residues 733 to 751 of CYFIP1 may fold into an eIF4E-binding domain even though the amino acid sequence does not conform to the previously established consensus YxxxxLL (Mader et al., 1995; Altmann et al., 1997). The charged residues implicated in the interaction are important for establishing the recognition between CYFIP1 and eIF4E. Interestingly, this pattern is common among three different protein families (CYFIP, 4G, 4E-BPs) that interact with eIF4E (Figure 2A).

To determine whether CYFIP1 is a 4E-BP, we performed GST-Sepharose pull-down assays using in vitro-synthesized ^{35}S-methionin-labeled proteins. Like 4E-T (Ferraiuolo et al., 2005) (Figure 3A, lane 7), CYFIP1 was precipitated specifically by GST-eIF4E (Figure 3A, compare lane 4 with lanes 2 and 3), indicating that eIF4E directly interacts with CYFIP1. The binding of CYFIP1 to the GST-eIF4E W73A mutant was reduced by 70%, similar to the effect on 4E-T (Figure 3B). eIF4E simultaneously interacts with CYFIP1 and m^7GTP, because both proteins were retained on m^7GTP-Sepharose beads. The retention of CYFIP1 was insensitive to RNase and DNase (Figure S5). To verify the importance of the putative eIF4E-binding region for the eIF4E-CYFIP1 interaction, we introduced several mutations in the CYFIP1 sequence (Figure 3C), followed by chromatography on m^7GTP-Sepharose (Figure 3D). First, the Asp742 and Arg744 residues were both mutated to alanine, thus removing the salt bridge at the beginning of the α helix and presumably allowing more flexibility of the critical Lys743. This mutant (A-A) bound 20% less efficiently than did the wild-type. We introduced other mutations that affect both internal salt bridges (Asp742Lys; Arg744Glu; Glu748Lys) and invert the electric charge of the critical lysine that is predicted to interact with eIF4E (Lys743Glu). Binding of this quadruple mutant (KEE-K) was reduced even further (by 60%), indicating that this region of CYFIP1 is involved in eIF4E binding. Finally, we studied the importance of the lysine that presumably interacts with eIF4E, mutating it to glutamate (-E-). This single substitution had an effect similar to that of the quadruple mutation; a reduction of 70% (compare the last two bars in Figure 3D, right panel). Because the substitution of Lys743 with a residue of opposite charge did not induce destabilization of the "reverse L shaped" structure of the CYFIP1 peptide, the strong inhibition of eIF4E binding indicates that Lys743 is involved in the interaction of CYFIP1 with eIF4E, as predicted by sequence and structural analysis (Figure S6). On the contrary, the two salt bridges, Asp742-Arg744 and Glu748-Lys750 (Figure 2A), stabilize the CYFIP1 peptide in a conformation that is able to interact with the eIF4E protein surface through Lys743. Mutagenesis of CYFIP1 where a 4E-BP motif similar to the YxxxxLL consensus was found (WFREFFL) (Figure S7) did not significantly change the binding to eIF4E.

To assess whether the isolated CYFIP1 peptide, which includes the eIF4E-binding domain, binds purified eIF4E, we synthesized wild-type (WT) and two mutant peptides (K-EE-K and -E-, Figure 3C) affixed to biotin. The western blot in Figure 3E shows that under stringent conditions (300 mM NaCl), no eIF4E bound to either the control (lane 2) or the CYFIP1 mutant peptides (lanes 4 and 5), whereas the streptavidin beads containing the WT peptide efficiently bound purified human eIF4E (lane 3). In less stringent conditions (150 mM NaCl, lower panel) the mutant peptides also bound some eIF4E but with lower efficiency than did the WT peptide. Therefore, the region of CYFIP1 with structural homology to the 4E-BPs does indeed bind eIF4E. CYFIP1 specifically and directly interacts with eIF4E through the noncanonical motif DKRLRSECK, where the lysine at the second position is critical for the interaction.

The FMRP-CYFIP1 Complex Is Consolidated by Binding to RNAs

To address the role of CYFIP1 in vivo, we transfected mammalian cells with DNA encoding this protein; as expected, overexpression of CYFIP1 repressed general translation. Silencing of CYFIP1 increased general translation (Figure S8B). Targeting

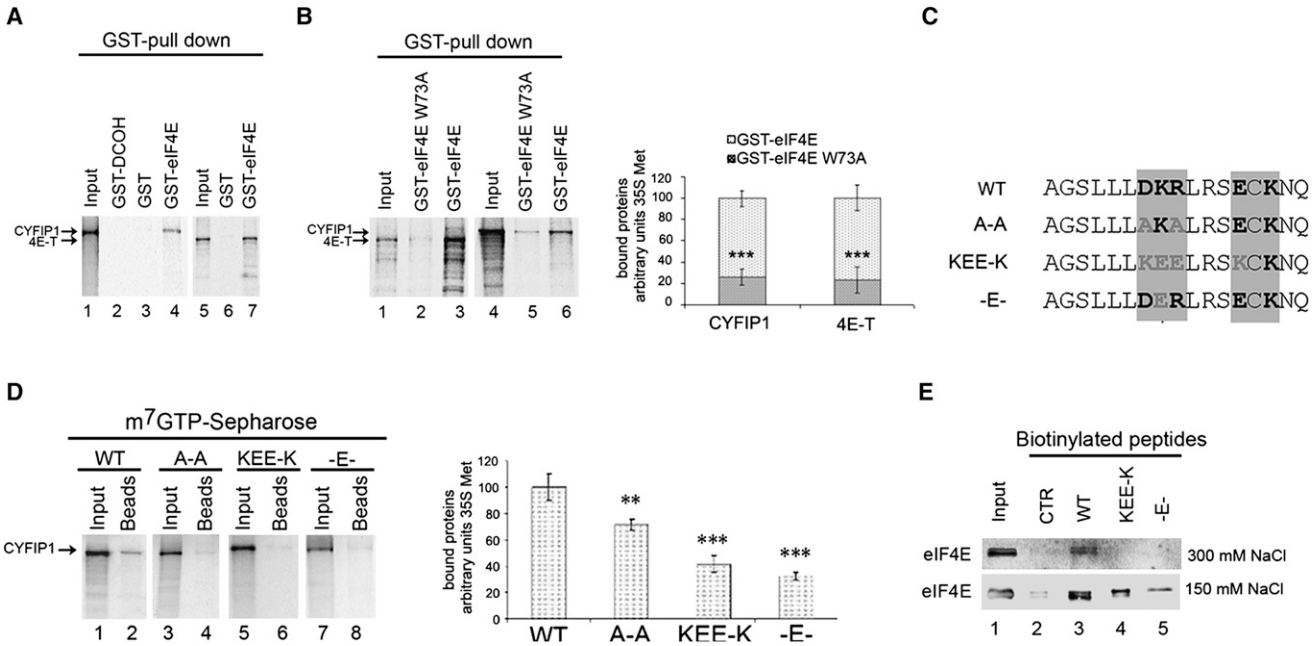

Figure 3. eIF4E and CYFIP1 Interact Directly

(A) GST pull-down assays. *E. coli*-expressed GST, GST-DCOH, and GST-eIF4E were immobilized on glutathione-Sepharose and incubated with ^{35}S-methionine-labeled CYFIP1 and 4E-T. Lanes 1 and 5, inputs. GST-eIF4E bound CYFIP1 (compare lanes 2–4) and 4E-T (positive control, lane 7).

(B) GST fusion protein binding assays. GST-eIF4EW73A mutant protein (lanes 2 and 5) or wild-type eIF4E (lanes 3 and 6) was incubated with ^{35}S-methionine-labeled 4E-T or CYFIP1 proteins. The relative intensities of CYFIP1 or 4E-T (bound proteins:input) were quantified. Proteins bound to GST-eIF4E W73A (dark gray bars) were compared to proteins bound to GST-eIF4E (100% binding, light-gray bars) (n = 5) ***$p < 0.001$, Student's t test.

(C) CYFIP1 amino acid sequence of the WT and mutant eIF4E-binding peptide. A-A, KEE-K, and -E- mutants are shown.

(D) m^{7}GTP binding assays. ^{35}S-methionine-labeled wild-type or mutant CYFIP1 was applied to m^{7}GTP-sepharose beads. Lanes 1, 3, 5, and 7 represent the input of WT and mutant CYFIP1 proteins, respectively (1/10). Lanes 2, 4, 6, and 8 represent the CYFIP1 proteins bound to m^{7}GTP beads. Relative intensities (bound: input) of WT and CYFIP1 mutants were quantified as described before (n = 8). ***$p < 0.001$, **$p < 0.01$, ANOVA and Dunnett's multiple comparison tests.

(E) Peptide binding assay. Human GST-eIF4E was applied to streptavidin beads containing wild-type or mutant CYFIP1 biotinylated peptides (sequences in [C]) or unrelated peptide with a biotin added to the N terminus. The bound eIF-4E was detected by immunoblotting. Lane 1, input (1/20); lane 2, unrelated peptide; lane 3, WT peptide; and lanes 4 and 5, K-EE-K and -E- mutant peptides, respectively.

of CYFIP1 to a specific mRNA further reduces its expression (Figures S8A–S8C).

According to our model, FMRP recruits CYFIP1 to mRNAs. To test this model, we used ^{35}S-labeled FMRP and CYFIP1 proteins and the FMRP target mRNA encoding *Arc/Arg3.1*. GST-eIF4E pull-down experiments showed that eIF4E did not bind significantly to FMRP (Figure 4A, compare lane 3 with lane 7), whereas it binds to CYFIP1, as shown before (compare lane 4 to lane 8). When capped-*Arc* mRNA was added, CYFIP1 and especially FMRP interacted more efficiently with eIF4E (Figure 4A, lane 6). The specificity was confirmed by the reduced recovery of the FMRP-CYFIP1 complex in presence of a nonneuronal mRNA (capped-*luciferase* mRNA), as shown in Figure 4A (lane 10). Some residual FMRP and CYFIP1 bound also to *luciferase* mRNA, in agreement with the fact that CYFIP1 also inhibits *luciferase* mRNA (by 25%; Figure S8). Thus, the interaction between FMRP/CYFIP1 and eIF4E is increased and possibly stabilized by the presence of target mRNAs, consistent with the decreased coprecipitation of FMRP with CYFIP1 after RNase treatment (Figure 1D).

Blocking of BC1 RNA in vitro reduces the affinity of FMRP to at least some of its target mRNAs (Zalfa et al., 2003). We therefore tested whether the absence of *BC1* RNA interferes with the binding of FMRP-CYFIP1 to eIF4E. When m^{7}GTP-Sepharose and brain extracts from *BC1* KO mice were used, there was a significant decrease (by 60%) in the amount of recovered FMRP (Figure 4B, lane 7). This effect is consistent with the decreased coprecipitation of FMRP with CYFIP1 after RNase treatment (Figure 1D). Furthermore, CYFIP1 formed an RNP containing *BC1* RNA (Figure 4B and Figure S9), and in the absence of FMRP, the association of *BC1* RNA with CYFIP1 decreased (Figure 4C), indicating that FMRP and *BC1* require each other for optimal interaction with CYFIP1 and eIF4E.

We then assessed whether CYFIP1 is associated with mRNAs in the brain. Figure 4D (lanes 2 and 3) shows that *Map1b* mRNA (Bagni and Greenough, 2005) was detected in the CYFIP1 immunoprecipitate. One negative control was neuronal *D$_2$DR* mRNA, whose metabolism is not affected by FMRP (Centonze et al., 2007a). Other FMRP target mRNAs were also investigated. The association of *Map1b*, *αCaMKII*, and *Arc* (Zalfa et al., 2003), but possibly not of *App* (Westmark and Malter, 2007), with the CYFIP1 complex was decreased in the absence of BC1 RNA (Figure 4D, Figure S9). RT-Q-PCR was also performed for *Map1b* mRNA (Figure 4E), confirming and extending our previous data

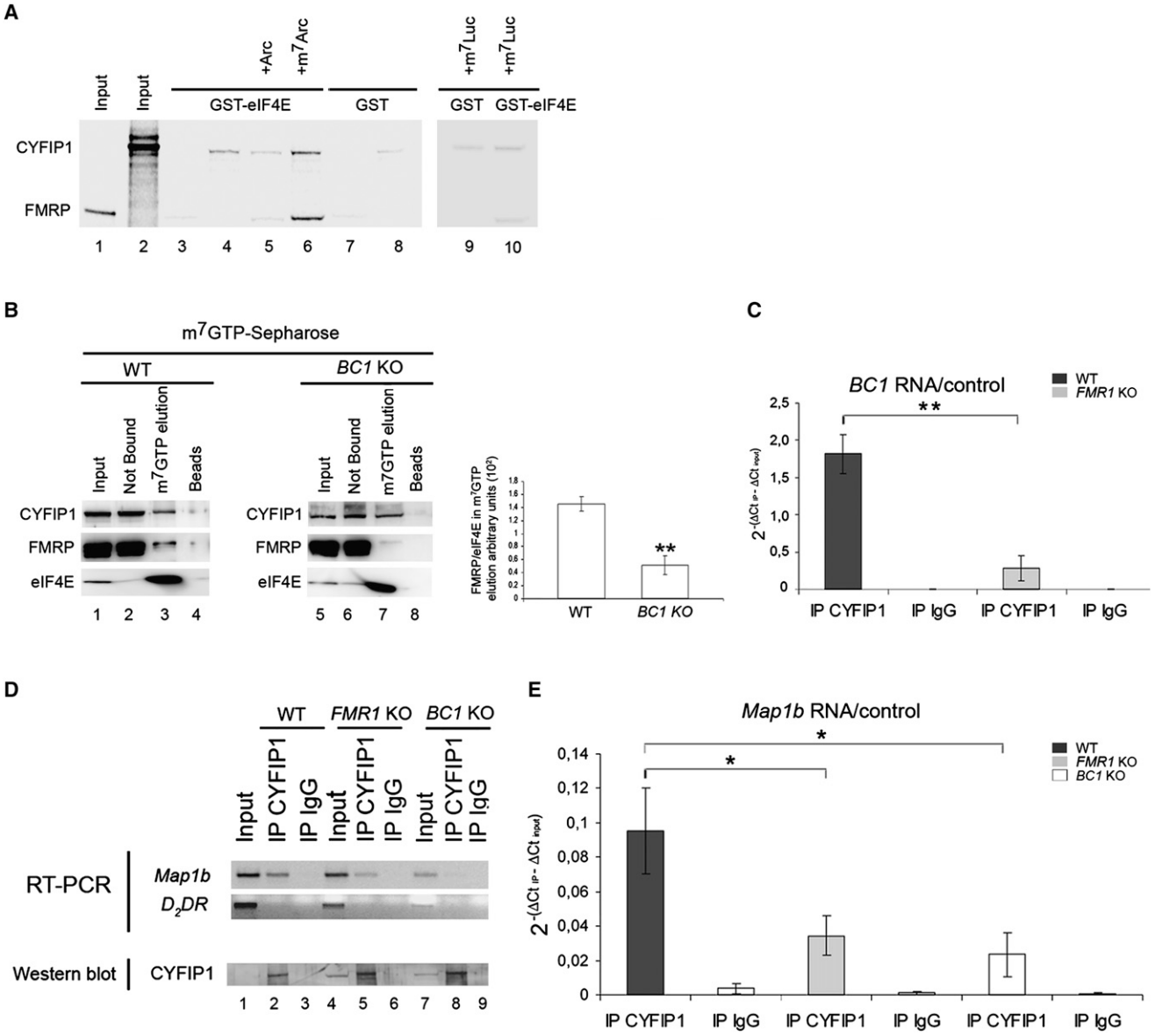

Figure 4. RNA Facilitates CYFIP1-FMRP Complex Formation

(A) *Arc* mRNA facilitates the CYFIP1-FMRP-eIF4E complex formation. Lanes 1 and 2, inputs (1/10) of ^{35}S-methionine-labeled FMRP and CYFIP1; lane 3, FMRP binding to the GST-eIF4E; lane 4, CYFIP1 binding to GST-eIF4E; lane 5, FMRP + CYFIP1 binding to GST-eIF4E in presence of uncapped *Arc* mRNA; lane 6, FMRP + CYFIP binding to the GST-eIF4E in the presence of m^{7}G-capped *Arc* mRNA; lane 7, FMRP binding to GST; lane 8, CYFIP1 binding to GST; lane 9, FMRP + CYFIP1 binding to GST in the presence of firefly m^{7}G-capped *luciferase* mRNA; and lane 10, FMRP + CYFIP1 binding to GST-eIF4E in the presence of firefly m^{7}G-capped *luciferase* mRNA.

(B) *BC1* RNA increases eIF4E-CYFIP1-FMRP complex formation. Extracts from WT or *BC1* KO brains were incubated with m^{7}GTP-Sepharose and m^{7}GTP-eluted proteins were separated by SDS-PAGE. CYFIP1, FMRP, and eIF4E were detected by immunoblotting. Lanes 1 and 5, inputs (1/20), lanes 2 and 6, unbound proteins (1/20); lanes 3 and 7, specific elution with free m^{7}GTP; and lanes 4 and 8, proteins bound to the beads after specific elution. The level of FMRP was normalized for the amount of eIF4E in the specific elution (lanes 3 and 7). Average of independent experiments is plotted on the histogram (n = 6, right panel). **p < 0.01, Student's t test.

(C) CYFIP1 is part of a neuronal RNP. RT-Q-PCR of *BC1* RNA from wild-type (WT) and *FMR1* KO brain extracts was performed after CYFIP1 or IgG immunoprecipitation (n = 4). **p < 0.01, Student's t test.

(D) After CYFIP1 immunoprecipitation from WT, *FMR1*, and *BC1* KO brain extracts, the RNA was extracted, and RT-PCR was used to detect *Map1b* and *D$_2$DR* mRNAs. Lanes 1, 4, and 7 represent the inputs (1/10). Lanes 2, 5, and 8 contain the immunoprecipitated RNA from WT, *FMR1*, and *BC1* KO extracts, respectively. Lanes 3, 6, and 9 reflect the mRNA associated with the control rabbit IgG. Lower panel: a western blot from the immunoprecipitated CYFIP1 performed from one-fourth of the same experiment used for the RT-PCR.

(E) RT-Q-PCR of CYFIP1-associated *Map1b* mRNA. RT-Q-PCR of *Map1b* from WT, *FMR1*, and *BC1* KO brain extracts was performed after CYFIP1 or control IgG immunoprecipitation (n = 7). *p < 0.05, ANOVA and Dunnett's multiple comparison tests.

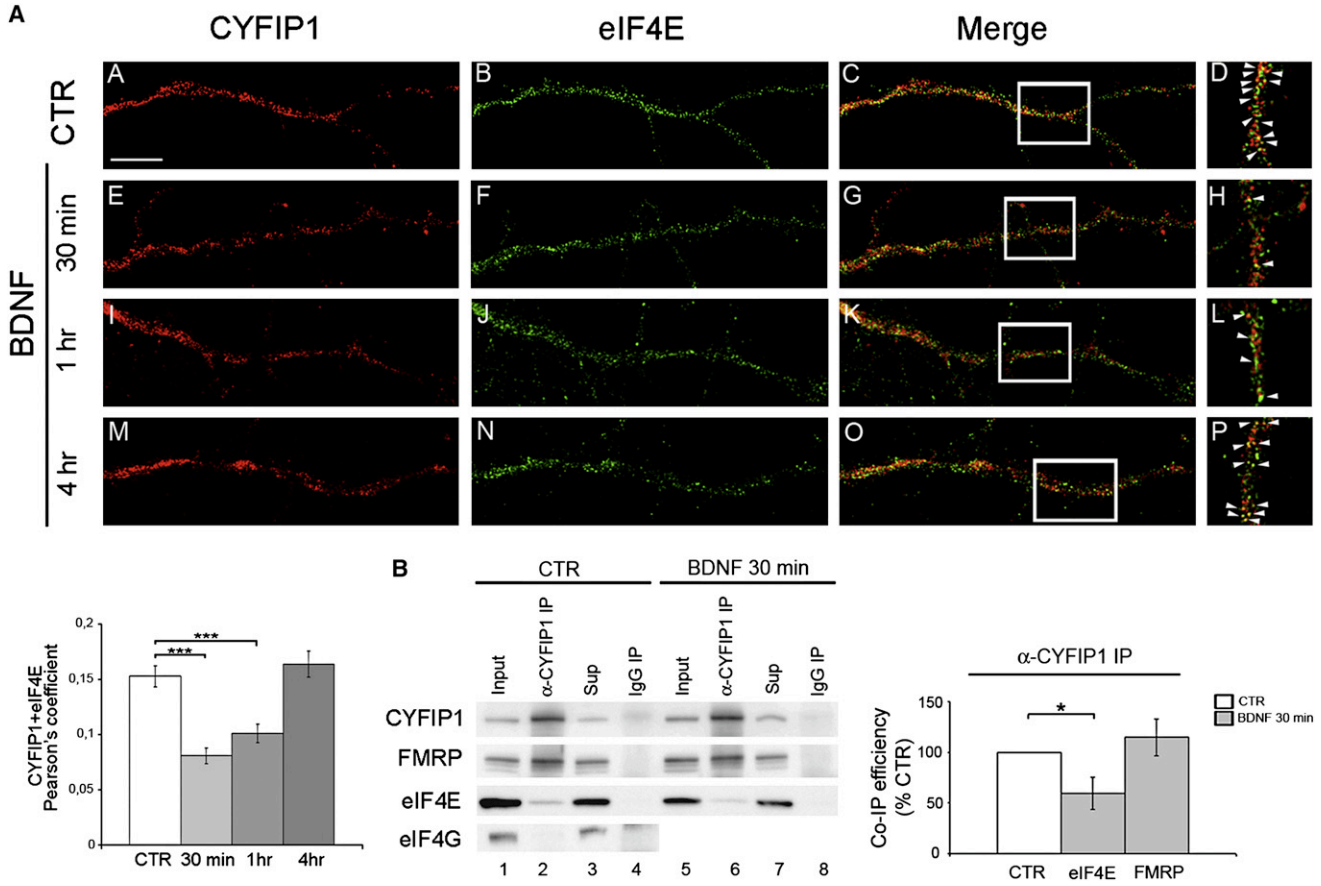

Figure 5. The CYFIP1-eIF4E Complex Is Activity-Regulated

(A) CYFIP1-eIF4E colocalization in dendrites under resting and stimulated conditions. Cortical neurons (14 DIV) were stained for CYFIP1 (red) and eIF4E (green) (colocalization is in yellow) under control conditions (CTR) (subpanels A–D) or after BDNF stimulation (subpanels E–P) at three different times. Subpanels D, H, L, and P show enlargements of the areas boxed in white with white arrowheads pointing to colocalization of CYFIP1 and eIF4E. Quantification of four independent experiments (a total of 320 neurites for each condition) was performed with the ImageJ program package and reported as a histogram. ANOVA, post hoc Scheffè test; ***$p < 0.0001$ and ***$p < 0.001$ at 30 min and 1 hr, respectively, and $p = 0.99$ at 4 hr. The scale bar represents 10 μm.

(B) CYFIP1-eIF4E-FMRP association in resting and stimulated neuronal cultures. CYFIP1 was immunoprecipitated under control conditions (lane 2, bottom panel) or after BDNF treatment (lane 6), and its presence with eIF4E and FMRP was analyzed by western blotting. Under control conditions, eIF4G was absent from the complex (lane 2). Quantification of eight independent experiments to detect eIF4E and four to detect FMRP is reported in the histogram. The amount of coimmunoprecipitated eIF4E or FMRP was normalized for the immunoprecipitated CYFIP1. *$p < 0.05$, one-sample Student's t test.

that a significant (60%) decrease in the association of this transcript with CYFIP1 occurred in *BC1* KO mice. Another putative FMRP target is *Fmr1* mRNA (Schaeffer et al., 2001; Miyashiro et al., 2003), which we did not detect in the neuronal CYFIP1 complex (Figure S9). Taken together, these data show that CYFIP1 requires *BC1* RNA and FMRP for optimal association with—and translational repression of—some key brain mRNAs.

The FMRP-CYFIP1 Complex Is Activity-Regulated in Neurons

Next, we analyzed the distribution of FMRP-CYFIP1, FMRP-eIF4E, and CYFIP1-eIF4E in primary cultures of hippocampal neurons. eIF4E was colocalized with CYFIP1 and FMRP in cell bodies and dendrites (Figure S10; see Figure S11 for specificity of antibody reaction). In some cases, synaptic activity and/or developmental transitions can alleviate translational repression (Gebauer and Hentze, 2004; Richter and Sonenberg, 2005); consequently, we investigated whether BDNF stimulation caused release of eIF4E from the FMRP-CYFIP1 complex. Resting neuronal cultures are shown in Figure 5A, subpanels A–D. BDNF was added to hippocampal neurons for 30 min, 1 hr, or 4 hr, followed by eIF4E and CYFIP1 immunodetection (Figure 5A, subpanels E–P). The overlap of CYFIP1 and eIF4E signals changed significantly with BDNF treatment; it decreased by 30% after 1 hr of treatment. Over 4 hr, however, the difference from baseline was not significant (Figure 5A, subpanels M–P). To verify that the diminished colocalization corresponded to a decrease in the CYFIP1-eIF4E complex, we performed CYFIP1 immunoprecipitations with similarly treated neurons (Figure 5B). As expected, the yield of coprecipitating eIF4E, normalized for the amount of precipitated CYFIP1, was reduced (by 40%) after 30 min of BDNF treatment, although FMRP levels did not change (Figure 5B). These data suggest that diminished colocalization reflects a decrease in complex formation. Moreover, eIF4G did

not coprecipitate with CYFIP1 (Figure 5B, bottom panel), further indicating that CYFIP1, like other 4E-BPs, competes with eIF4G for binding to eIF4E. These observations indicate that the inhibitory FMRP-CYFIP1-eIF4E complex is dynamically regulated in an activity-dependent manner to repress and then possibly release dendritic mRNAs for translation.

The FMRP-CYFIP1-eIF4E Complex Is Present and Active at Synapses

To address the functional significance of the FMRP-CYFIP1-eIF4E complex at synapses, we prepared synaptoneurosomes (Pilo Boyl et al., 2007), the enrichment of which was monitored by PSD-95 levels in the synaptic fraction compared to total extracts (Figure S12). m^7GTP-Sepharose beads were then incubated with extracts from cortical synaptoneurosomes. Figure 6A shows that CYFIP1 bound to the beads was specifically eluted with m^7GTP, and FMRP was also detected in this complex (Figure 6A, lane 3).

We then stimulated cortical synaptoneurosomes with BDNF, immunoprecipitated CYFIP1, and examined coprecipitated eIF4E or associated mRNAs. In control experiments, eIF4E was associated with CYFIP1 (Figure 6B, lane 2). After 30 min of BDNF stimulation, a fraction of the eIF4E was released from the CYFIP1 complex (Figure 6B, lane 5 and right panel). The disassembly of the CYFIP1-eIF4E complex suggests that target mRNA translation was activated; indeed, around 80% of *Map1b* and *BC1* RNAs, as measured by RT-Q-PCR, was released from the CYFIP1 complex after stimulation (Figure 6C).

Because FMRP responds to mGluR stimulation (Weiler et al., 1997; Huber et al., 2002; Dolen et al., 2007), we treated hippocampal and cortical synaptoneurosomes with the group I mGluR agonist DHPG. After 5 min of stimulation, a significant decrease of eIF4E in the CYFIP1 complex was observed (Figure 6D). Longer stimulations (DHPG for 15 min) caused a significant increase in CYFIP1-eIF4E complex formation (Figure S13), suggesting that mGluR stimulation induced an initial release of CYFIP1-eIF4E-regulated translation followed by rapid overcompensation. We also electroporated primary cortical neurons with siRNAs directed against *CYFIP1*; reduction of CYFIP1 protein lead to an increase of MAP1B (Figure S14). Finally, extracts from *CYFIP1* heterozygote mice (*CYFIP1*$^{+/-}$) were analyzed; in this case, MAP1B protein increased by ~25% compared to the WT. Furthermore, the translation of αCaMKII and APP proteins was also upregulated by ~70% and ~90%, respectively (Figure 6E, compare lanes 1 and 2). Taken together, these data show that CYFIP1 regulates the expression of *Map1b* and other FMRP target mRNAs.

DISCUSSION

Although CYFIP1 was identified as an FMRP-interacting factor as well as a component of the WAVE complex involved in actin polymerization, its molecular function was unknown (Schenck et al., 2001; Kunda et al., 2003). We show that CYFIP1 binds eIF4E in brain extracts, synaptoneurosomes (Figures 1 and 6), and in vitro (Figure 3A). CYFIP1 contains a peptide that is predicted to exhibit structural similarity to the canonical eIF4E-binding domain (Richter and Sonenberg, 2005) (Figure 2A). Indeed, the integrity of this sequence motif is required for efficient eIF4E binding (Figures 3C–3E). CYFIP1 is not the first eIF4E-binding protein that does not contain a well-conserved eIF4E-binding peptide; the *Xenopus* oocyte maturation factor Maskin (Richter and Sonenberg, 2005) is another example. It seems therefore likely that by convergent evolution, several protein families developed a surface domain that can efficiently block access of eIF4G to eIF4E.

FMRP Recruitment of CYFIP1 Represses Translation

The 4E-BPs bind eIF4E independently of other factors and thus downregulate the translation of many mRNAs that have no obvious sequence similarity (Richter and Sonenberg, 2005). In other cases, eIF4E-binding proteins are recruited by specific proteins present only on a subset of mRNAs. For example, Maskin requires the RNA binding protein CPEB (Richter and Sonenberg, 2005), and Cup requires Bruno (Nakamura et al., 2004) or other proteins (Nelson et al., 2004), depending on the developmental stage. Here, we show that CYFIP1 inhibits the translation of associated mRNAs through FMRP (Figure 4). We propose that in the brain, FMRP helps recruit and/or stabilize CYFIP1 on the 5′ end of specific mRNAs to repress translation. Several observations support this point: the two proteins form a heterodimer (Schenck et al., 2001); FMRP increases the affinity of CYFIP1 for capped mRNAs (Figure 4A); *BC1*, an RNA involved in FMRP-mRNA complex formation (Zalfa et al., 2003, 2005; Gabus et al., 2004), also increases the FMRP-CYFIP1-eIF4E interaction (Figure 4B); CYFIP1 is associated with *BC1* RNA, *Map1b*, *αCaMKII*, *Arc*, and *App* mRNAs in the brain; in *FMR1* or *BC1* KO mice, the interaction of these mRNAs with CYFIP1 is decreased (Figures 4C–4E, Figure S9, and data not shown). Finally, reduction of CYFIP1 in the brain leads to an increase of MAP1B, APP, and αCaMKII (Figure 6E). These increases are consistent with those observed in the absence of FMRP in the mammalian brain (Zhang et al., 2001; Zalfa et al., 2003; Lu et al., 2004; Hou et al., 2006; Westmark and Malter, 2007). *Fmr1* mRNA, an FMRP target (Schaeffer et al., 2001; Miyashiro et al., 2003), is not part of the CYFIP1 mRNP, and consequently FMRP expression does not change upon CYFIP1 reduction (Figure 6E and Figures S9 and S14). Perhaps *Fmr1* mRNA is regulated by a different FMRP complex or is not controlled at the translational level.

The FMRP-CYFIP1-eIF4E Complex Responds to Synaptic Stimulation

One major issue concerning translation in neurons is regulation by synaptic stimulation. Protein synthesis is activated by several synaptic stimuli such as BDNF and DHPG. BDNF stimulates translation via mTOR and ERK-MAPK at synapses and likely involves modulation of initiation. Moreover, BDNF activates the translation of *Arc* and *αCaMKII* mRNAs in dendrites and at synapses (Aakalu et al., 2001; Yin et al., 2002; Schratt et al., 2004). After application of BDNF to cultured primary neurons and synaptoneurosomes, we observed a dissociation of eIF4E and CYFIP1, which coincided with the release of associated (m)RNAs (Figures 5, 6B, and 6C). In our model (Figure 7), this disassembly would free eIF4E to initiate translation.

DHPG stimulation of mGluR activity also induces translation initiation via ERK and subsequent eIF4E phosphorylation (Richter and Klann, 2007). DHPG stimulation of synaptoneurosomes

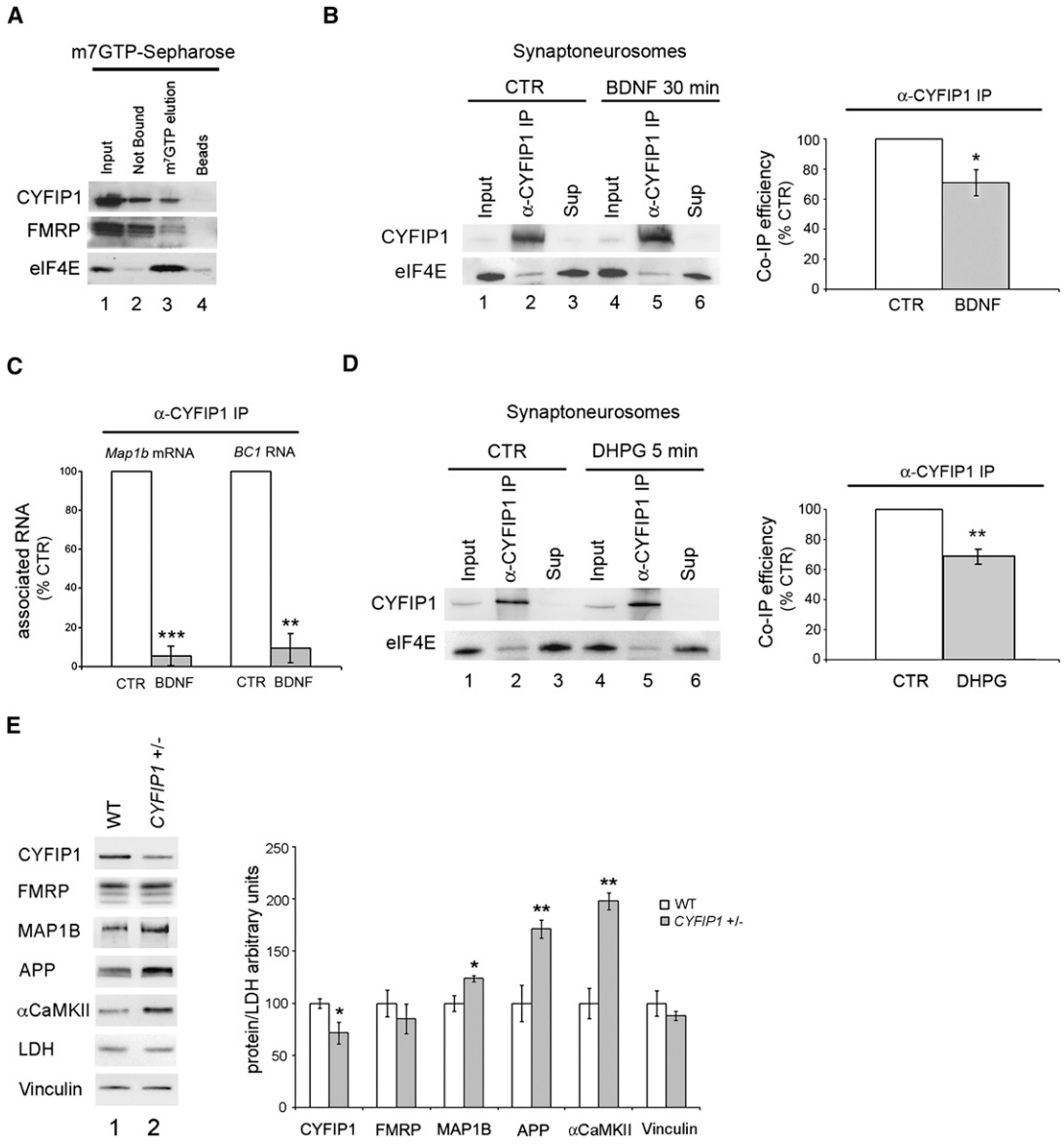

Figure 6. The FMRP-CYFIP1-eIF4E Complex Is Activity Regulated at Synapses

(A) CYFIP1-eIF4E complex is detected in synaptoneurosomes. m^7GTP-Sepharose beads were incubated with synaptic extracts; the recovered proteins were immunoblotted for CYFIP1, FMRP, and eIF4E. Lane 1, input (1/20); lane 2, unbound proteins; lane 3, specific elution with free m^7GTP; and lane 4, proteins bound to the beads after specific elution (beads).

(B) The CYFIP1-eIF4E complex is activity regulated at synapses. Proteins coimmunoprecipitating with CYFIP1 (lanes 2 and 5), respective supernatants (lanes 3 and 6), and inputs (1/40, lanes 1 and 4) were analyzed by immunoblotting. Quantification of four independent experiments is represented in the histogram. *$p < 0.05$, one-sample Student's t test.

(C) CYFIP1 is part of a synaptic BDNF-sensitive mRNP complex. Shown is the amount of *Map1b* mRNA and *BC1* RNA, as determined by RT-Q-PCR, that coprecipitates with CYFIP1 after mock or BDNF stimulation of synaptoneurosomes (n = 4). Values were normalized for the mock control of each experiment. ***$p < 0.001$, **$p < 0.01$, one-sample Student's t test.

(D) eIF4E is released from the CYFIP1 complex after DHPG stimulation. The experiments were performed as in (B) with DHPG stimulation for 5 min. n = 5, **$p < 0.01$, one-sample Student's t test.

(E) CYFIP1 affects protein levels encoded by some FMRP target mRNAs. Brain proteins from WT (lane 1) or CYFIP1$^{+/-}$ mice (lane 2) were analyzed by immunoblotting to detect CYFIP1, FMRP, MAP1B, APP, αCaMKII, LDH, and vinculin levels (left panel). Quantified proteins were normalized for LDH. This ratio in WT mice was set at 100%. Histogram in the right panel shows the quantification of five independent experiments. **$p < 0.01$, *$p < 0.05$, Student's t test.

caused CYFIP1-eIF4E dissociation (Figure 6D), confirming a response of FMRP translational repression to mGluR signaling (Huber et al., 2002; Hou et al., 2006; Dolen et al., 2007). Interestingly, we detected the release of CYFIP1 from eIF4E only after a short stimulation (Figure 6D), which could be due to a short pulse of FMRP dephosphorylation observed under similar

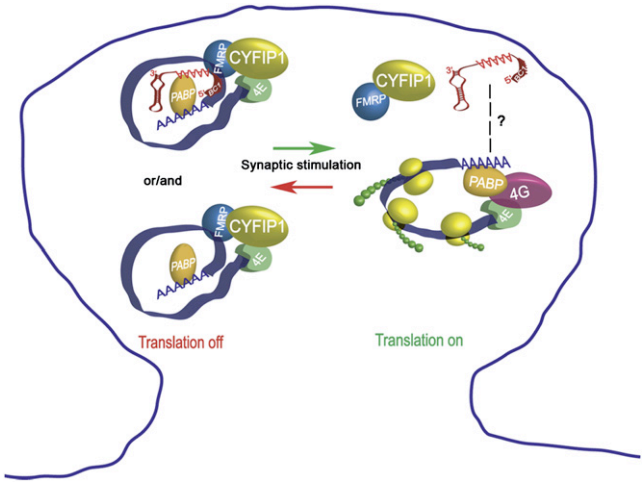

Figure 7. Proposed Model for mRNA Translational Repression and Activation by the CYFIP1-FMRP Complex

The CYFIP1-FMRP or CYFIP1-FMRP-*BC1* mRNA complex is transported in dendrites as translationally silent mRNPs. Some of these mRNPs are also present at synapses. After synaptic stimulation, and possibly after CYFIP1 and/or FMRP protein modifications, the CYFIP1-FMRP complex is released from eIF4E, and local mRNA translation ensues.

conditions (Narayanan et al., 2007). Alternatively, because Rac1 in its GTP form disassembles the FMRP-CYFIP1 complex in *Drosophila* (Schenck et al., 2003), it is tempting to speculate that a similar mechanism could also mediate eIF4E dissociation from CYFIP1.

Relevance for the Fragile X Syndrome

We propose that in the absence of FMRP, which causes FXS, there would be decreased binding of CYFIP1 to FMRP target mRNAs. This would relieve translational suppression and induce higher than normal levels of proteins whose synthesis is under the control of FMRP. On the other hand, the fact that CYFIP1 associates with the WAVE complex, which plays a role in actin polymerization (Bogdan et al., 2004), implicates the FMRP regulatory complex in synapse maturation. In support of this notion, synaptic abnormalities observed in mutants affecting Rac1 signaling pathways resemble those in the FXS (Tashiro and Yuste, 2004). Furthermore, the role of CYFIP1 as coregulator of FMRP may also help to explain the autistic features of FXS because CYFIP1 has been recently implicated in autism (Nishimura et al., 2007; Nowicki et al., 2007). Further work is needed to understand the functional consequences of impaired local protein synthesis in the developing brain and how this correlates to the autistic and FXS phenotypes.

EXPERIMENTAL PROCEDURES

Animals

All animals were treated according to institutional and international guidelines (see the Supplemental Data). The C57/BL6 *FMR1* KO mice were provided by Ben Oostra (Bakker et al., 1994), the 129Sv *BC1* KO mice by Juergen Brosius (Skryabin et al., 2003), and the CYFIP1$^{+/-}$ mice by Walter Witke (M.M. and W.W., unpublished data). All of the animals used in this study were 3 weeks old.

GST Pull-Down Assay

Plasmids encoding GST, GST-DCOH, GST-eIF4E, and GST-eIF4E Trp73Ala (see the Supplemental Data) were expressed in *E. coli* BL21; lysates were clarified and mixed with glutathione-Sepharose 4B beads (Amersham-Biosciences) for 1 hr at 4°C. The beads were collected and washed in PBS 1×. Glutathione beads containing the same amount of fusion proteins (5–10 μg) were incubated in binding buffer (20 mM Tris-HCl [pH 8.0], 100 or 200 mM NaCl, 1 mM ethylenediaminetetraacetic acid [EDTA], and 0.5% NP-40). Proteins bound to the beads were resolved by SDS-PAGE. The same amounts of protein were subsequently incubated in 250 μl of binding buffer in the presence of 5 μl of lysate containing in vitro-synthesized protein (TNT System Promega). After 90 min incubation at 4°C, the beads were washed in binding buffer and resolved by SDS-PAGE and phosphorimaged.

Protein Extract Preparation

Total mouse brain and cultured primary neurons were homogenized in lysis buffer (100 mM NaCl, 10 mM $MgCl_2$, 10 mM Tris-HCl [pH 7.5], 1 mM dithiothreitol, 30 U/ml RNasin, 1% Triton X-100, 0.5 mM Na-orthovanadate, 10 mM β-glycerophosphate, and 10 μg/ml Sigma protease inhibitor), incubated 5 min on ice, and centrifuged at 12,000 g for 8 min at 4°C, and the supernatant was used for immunoprecipitations and m^{7}GTP-Sepharose chromatography. For total protein analysis, brains were homogenized in Laemli buffer, boiled, and vortexed. The procedures were repeated five times.

Immunoprecipitation

Brain (500–800 μg) or cell (200 μg) extracts were used for immunoprecipitation experiments. For immunoprecipitation of FMRP, brains were prepared as described above, and a reversible immunoprecipitation system (Catch and Release v2.0, Upstate) was used. For CYFIP1, the lysis buffer contained 150 mM NaCl, 50 mM Tris-HCl (pH 8.0), 1.5% Triton X-100, and protease inhibitors (Sigma). The lysates were centrifuged first at 1000 rpm and then at 10,000 rpm, each for 10 min at 4°C. The extracts were incubated with 4 μg of CYFIP1 polyclonal antibody (see Table S1 for antibodies) overnight at 4°C. Twenty microliters of protein A Sepharose (Amersham) previously saturated with 1% BSA in PBS was incubated with the extract for 90 min at 4°C. The beads were washed three times in 1 ml of buffer (150 mM NaCl, 50 mM Tris-HCl [pH 8.0], and 1% Triton X-100). The same amount of rabbit IgG was used as control. Immunoprecipitation experiments with CYFIP1 antibody followed BDNF (30 ng/ml) stimulation of cortical neurons for 30 min before collecting the cells.

Cosedimentation of Proteins on Polysome-mRNPs Gradients

Total mouse brain was homogenized in lysis buffer (see Protein Extract Preparation). The supernatants were centrifuged through 5%–25% sucrose gradients as described in the Supplemental Data. Fractions were analyzed by immunoblotting.

m^{7}GTP Chromatography

m^{7}GTP-Sepharose beads (Amersham Biosciences) were equilibrated with buffer A (100 or 200 mM KCl, 50 mM Tris-HCl [pH 7.5], 5–10 mM $MgCl_2$, and 0.5% Triton X-100) plus BSA (0.1 mg/ml) at 4°C for 30 min. The resin was washed and incubated with 500–900 μg of protein extract from mouse brain for 60 min at 4°C; GTP (100 μM) was added to reduce nonspecific binding. The beads were washed with 0.4 ml of buffer A and then incubated for 30 min with 200 μM of m^{7}GTP. In some cases, 100 μg of RNase A (Sigma) and 1000 U of RNase T1 (Roche) per mg of protein were added (Nakamura et al., 2004).

Assay with Biotinylated Peptides

Biotinylated CYFIP1 wild-type ([Btn]AGSLLLDKRLRSECKNQ), mutant ([Btn]AGSLLLKEELRSKCKNQ; [Btn]AGSLLLDERLRSECKNQ), and control ([Btn]GSAPTRPPPLPP) peptides (Sigma) were dissolved in Tris-buffered saline (TBS)/Tween (0.02%); each peptide (25 μg) was incubated with streptavidin-conjugated magnetic beads (30 μl, Invitrogen) for 15 min at room temperature in buffer (150 or 300 mM NaCl, 50 mM Tris-HCl [pH 7.5], and 0.1% Triton X-100). The beads were then washed twice in the same buffer and mixed with

purified human GST-eIF4E (200 or 400 ng) for 1 hr at 4°C. The beads were then washed, and the protein was eluted, immunoblotted, and probed for eIF4E.

Immunoprecipitation Followed by RT-PCR and RT-Q-PCR Analysis

For RT-PCR and RT-Q-PCR analysis of immunoprecipitates, the beads were saturated in 1% BSA in PBS and heparin (1 mg/ml). CYFIP1 antibody was incubated with the beads (90 min at 4°C), washed three times (150 mM NaCl, 50 mM Tris-HCl [pH 8.0], and 1% Triton X-100), and incubated with 300 μg of brain extract or 200 μg of synaptic brain extract plus heparin (0.1 mg/ml) for 1 hr at 4°C. They were then washed, and RNA was eluted in 0.2 M NaAcetate, 1 mM EDTA, and 0.2% SDS for 5 min at 95°C. RNA was extracted (Trizol, Invitrogen) and used for p(dN)6-primed RT and PCR with mRNA-specific primers (Table S2). Real-time PCR was performed with an ABI 7900 Sequence Detector with dual-labeled TaqMan probes (Applied Biosystems). See the Supplemental Data for further details.

Neuronal Culture, Stimulation, and Image Analysis

Primary mouse cortical neurons (E15) were prepared as described (Ferrari et al., 2007); 14 DIV cells were treated with brain-derived neurotrophic factor (BDNF) (30 ng/ml, Alomone Laboratory) for 30, 60, or 240 min as described (Takei et al., 2001). They were then fixed with paraformaldehyde (1%–4%), permeabilized with Triton X-100 (0.2%), and analyzed for CYFIP1 and eIF4E. See Table S1 for details of the antibodies. The images were acquired with a confocal laser scanning microscope (LSM510, Zeiss and BIORAD Radiance 2010) with plan neofluar 40× or 63× oil objectives. Quantitative analysis in double-labeled material was performed blind from four different stimulated cultures by counting of 80 cells and 20 neurons (for each condition). A total of 320 dendrites over a length of 50 μm starting 20 μm from the nucleus was analyzed. Quantification was performed with ImageJ program (1.37v version) (from ImageJ for microscopy: http://www.macbiophotonics.ca/imagej/colour_analysis.htm#coloc_ica). See the Supplemental Data for further details.

Synaptoneurosomes

Synaptoneurosomes were prepared by homogenization of fresh cortex tissue in ice-cold buffer as described (Pilo Boyl et al., 2007). They were resuspended in HEPES-Krebs buffer (10 mM HEPES [pH 7.4], 150 mM NaCl, 3 mM KCl, 10 mM glucose, 2 mM $MgSO_4$, and 2 mM $CaCl_2$), equilibrated at 37°C for 5 min, and incubated at 37°C for 30 min with 200 ng/ml BDNF or for 5 min and 15 min with 100 μM DHPG. Stimulated and control (buffer treated) synaptoneurosomes were then lysed as previously described.

Homology Modeling Methods

A multialignment was carried out between a human 4E-BP1 fragment and twelve sequences of CYFIP 1 and 2, chosen among different species and isoforms (data not shown). In this multialignment, only the CYFIP sequences with a length comparable to that of human CYFIP1 were considered (KIAA0068, accession number D38549). A region showing a high conservation of residues that can be considered for the binding with eIF4E was found and modeled with the 4E-BP1 fragment present depicted by X-ray crystallography used as a template (Tomoo et al., 2005). The sequence numbering of CYFIP1 residues used throughout the analysis was made relative to the sequence of human CYFIP1 (accession number Q14467). See the Supplemental Data for further details.

Statistical Analysis

Differences between groups were determined by ANOVA and then Sheffé multiple comparison post hoc test, Dunnett's test, or one-sample Student's t test, where appropriate. Student's t test was used for comparisons where only two groups were analyzed. Correlations were determined with Pearson's correlation analysis. Significance was accepted at $p < 0.05$. Error bars represent the SEM.

SUPPLEMENTAL DATA

Supplemental Data include Supplemental Experimental Procedures, 14 figures, and two tables and can be found with this article online at http://www.cell.com/cgi/content/full/134/6/1042/DC1/.

ACKNOWLEDGMENTS

We thank Rasmus Herlo, Adriana Gambardella, and Emanuela Pasciuto for sharing preliminary data and Antonio Totaro and Caroline Lacoux for some help with protein purifications. We are grateful to Ben Oostra for the *FMR1* KO mice and to Jürgen Brosius for the *BC1* KO mice. We thank Kris Dickson for critical reading of the manuscript and discussion, Jesus Avila, Itzhak Fisher, and Gary Bassell for MAP1B antibodies, Stefano Biffo for eIF6/p27 antibody, Sebastian Munk for helping us with the confocal images, Nicola Gray and Fatima Gebauer for the MS2 reporter constructs, Oswald Steward for the full-length *Arc* cDNA, and Massimo Regoli for assistance with the statistical analysis. We thank Giorgio Bernardi for his support. M.M. was supported by a FP6 Marie Curie MEST-CT-2004-504640 fellowship. P.P.B. was partially supported by Conquer Fragile X Foundation. C.B. is supported by grants from the following agencies: Telethon (GGP05269), Ministero della Sanità e dell' Università (FIRB), and Flanders Interuniversity Institute for Biotechnology (VIB).

Received: March 27, 2007
Revised: April 25, 2008
Accepted: July 15, 2008
Published: September 18, 2008

REFERENCES

Aakalu, G., Smith, W.B., Nguyen, N., Jiang, C., and Schuman, E.M. (2001). Dynamic visualization of local protein synthesis in hippocampal neurons. Neuron *30*, 489–502.

Altmann, M., Schmitz, N., Berset, C., and Trachsel, H. (1997). A novel inhibitor of cap-dependent translation initiation in yeast: p20 competes with eIF4G for binding to eIF4E. EMBO J. *16*, 1114–1121.

Antar, L.N., Afroz, R., Dictenberg, J.B., Carroll, R.C., and Bassell, G.J. (2004). Metabotropic glutamate receptor activation regulates fragile x mental retardation protein and FMR1 mRNA localization differentially in dendrites and at synapses. J. Neurosci. *24*, 2648–2655.

Bagni, C., and Greenough, W.T. (2005). From mRNP trafficking to spine dysmorphogenesis: The roots of fragile X syndrome. Nat. Rev. Neurosci. *6*, 376–387.

Bakker, C.E., Verheij, C., Willemsen, R., Vanderhelm, R., Oerlemans, F., Vermey, M., Bygrave, A., Hoogeveen, A.T., Oostra, B.A., and Reyniers, E. (1994). Fmr1 knockout mice: A model to study fragile X mental retardation. Cell *78*, 23–33.

Banko, J.L., Merhav, M., Stern, E., Sonenberg, N., Rosenblum, K., and Klann, E. (2007). Behavioral alterations in mice lacking the translation repressor 4E–BP2. Neurobiol. Learn. Mem. *87*, 248–256.

Bogdan, S., Grewe, O., Strunk, M., Mertens, A., and Klambt, C. (2004). Sra-1 interacts with Kette and Wasp and is required for neuronal and bristle development in Drosophila. Development *131*, 3981–3989.

Centonze, D., Rossi, S., Napoli, I., Mercaldo, V., Lacoux, C., Ferrari, F., Ciotti, M.T., De Chiara, V., Prosperetti, C., Maccarrone, M., et al. (2007a). The brain cytoplasmic RNA BC1 regulates dopamine D2 receptor-mediated transmission in the striatum. J. Neurosci. *27*, 8885–8892.

Centonze, D., Rossi, S., Mercaldo, V., Napoli, I., Ciotti, M.T., Chiara, V.D., Musella, A., Prosperetti, C., Calabresi, P., Bernardi, G., and Bagni, C. (2007b). Abnormal Striatal GABA Transmission in the Mouse Model for the Fragile X Syndrome. Biol. Psychiatry *63*, 963–973.

Dolen, G., Osterweil, E., Rao, B.S., Smith, G.B., Auerbach, B.D., Chattarji, S., and Bear, M.F. (2007). Correction of fragile X syndrome in mice. Neuron *56*, 955–962.

Ferraiuolo, M.A., Basak, S., Dostie, J., Murray, E.L., Schoenberg, D.R., and Sonenberg, N. (2005). A role for the eIF4E-binding protein 4E-T in P-body formation and mRNA decay. J. Cell Biol. *170*, 913–924.

Ferrari, F., Mercaldo, V., Piccoli, G., Sala, C., Cannata, S., Achsel, T., and Bagni, C. (2007). The fragile X mental retardation protein-RNP granules

show an mGluR-dependent localization in the post-synaptic spines. Mol. Cell. Neurosci. *34*, 343–354.

Gabus, C., Mazroui, R., Tremblay, S., Khandjian, E.W., and Darlix, J.L. (2004). The fragile X mental retardation protein has nucleic acid chaperone properties. Nucleic Acids Res. *32*, 2129–2137.

Gebauer, F., and Hentze, M.W. (2004). Molecular mechanisms of translational control. Nat. Rev. Mol. Cell Biol. *5*, 827–835.

Gradi, A., Svitkin, Y.V., Imataka, H., and Sonenberg, N. (1998). Proteolysis of human eukaryotic translation initiation factor eIF4GII, but not eIF4GI, coincides with the shutoff of host protein synthesis after poliovirus infection. Proc. Natl. Acad. Sci. USA *95*, 11089–11094.

Haghighat, A., Mader, S., Pause, A., and Sonenberg, N. (1995). Repression of cap-dependent translation by 4E-binding protein 1: Competition with p220 for binding to eukaryotic initiation factor-4E. EMBO J. *14*, 5701–5709.

Hou, L., Antion, M.D., Hu, D., Spencer, C.M., Paylor, R., and Klann, E. (2006). Dynamic translational and proteasomal regulation of fragile X mental retardation protein controls mGluR-dependent long-term depression. Neuron *51*, 441–454.

Huber, K.M., Gallagher, S.M., Warren, S.T., and Bear, M.F. (2002). Altered synaptic plasticity in a mouse model of fragile X mental retardation. Proc. Natl. Acad. Sci. USA *99*, 7746–7750.

Johnson, E.M., Kinoshita, Y., Weinreb, D.B., Wortman, M.J., Simon, R., Khalili, K., Winckler, B., and Gordon, J. (2006). Role of Pur alpha in targeting mRNA to sites of translation in hippocampal neuronal dendrites. J. Neurosci. Res. *83*, 929–943.

Jung, M.Y., Lorenz, L., and Richter, J.D. (2006). Translational control by neuroguidin, a eukaryotic initiation factor 4E and CPEB binding protein. Mol. Cell. Biol. *26*, 4277–4287.

Kobayashi, K., Kuroda, S., Fukata, M., Nakamura, T., Nagase, T., Nomura, N., Matsuura, Y., Yoshida-Kubomura, N., Iwamatsu, A., and Kaibuchi, K. (1998). p140Sra-1 (specifically Rac1-associated protein) is a novel specific target for Rac1 small GTPase. J. Biol. Chem. *273*, 291–295.

Kunda, P., Craig, G., Dominguez, V., and Baum, B. (2003). Abi, Sra1, and Kette control the stability and localization of SCAR/WAVE to regulate the formation of actin-based protrusions. Curr. Biol. *13*, 1867–1875.

Lin, A.C., and Holt, C.E. (2008). Function and regulation of local axonal translation. Curr. Opin. Neurobiol. *18*, 60–68.

Lu, R., Wang, H., Liang, Z., Ku, L., O'Donnell, W.T., Li, W., Warren, S.T., and Feng, Y. (2004). The fragile X protein controls microtubule-associated protein 1B translation and microtubule stability in brain neuron development. Proc. Natl. Acad. Sci. USA *101*, 15201–15206.

Mader, S., Lee, H., Pause, A., and Sonenberg, N. (1995). The translation initiation factor eIF-4E binds to a common motif shared by the translation factor eIF-4 gamma and the translational repressors 4E-binding proteins. Mol. Cell. Biol. *15*, 4990–4997.

Marcotrigiano, J., Gingras, A.C., Sonenberg, N., and Burley, S.K. (1999). Cap-dependent translation initiation in eukaryotes is regulated by a molecular mimic of eIF4G. Mol. Cell *3*, 707–716.

Martin, K.C., Barad, M., and Kandel, E.R. (2000). Local protein synthesis and its role in synapse-specific plasticity. Curr. Opin. Neurobiol. *10*, 587–592.

Mazumder, B., Seshadri, V., and Fox, P.L. (2003). Translational control by the 3′-UTR: The ends specify the means. Trends Biochem. Sci. *28*, 91–98.

Miyashiro, K.Y., Beckel-Mitchener, A., Purk, T.P., Becker, K.G., Barret, T., Liu, L., Carbonetto, S., Weiler, I.J., Greenough, W.T., and Eberwine, J. (2003). RNA cargoes associating with FMRP reveal deficits in cellular functioning in Fmr1 null mice. Neuron *37*, 417–431.

Nakamura, A., Sato, K., and Hanyu-Nakamura, K. (2004). Drosophila cup is an eIF4E binding protein that associates with Bruno and regulates oskar mRNA translation in oogenesis. Dev. Cell *6*, 69–78.

Narayanan, U., Nalavadi, V., Nakamoto, M., Pallas, D.C., Ceman, S., Bassell, G.J., and Warren, S.T. (2007). FMRP phosphorylation reveals an immediate-early signaling pathway triggered by group I mGluR and mediated by PP2A. J. Neurosci. *27*, 14349–14357.

Nelson, M.R., Leidal, A.M., and Smibert, C.A. (2004). Drosophila Cup is an eIF4E-binding protein that functions in Smaug-mediated translational repression. EMBO J. *23*, 150–159.

Nishimura, Y., Martin, C.L., Vazquez-Lopez, A., Spence, S.J., Alvarez-Retuerto, A.I., Sigman, M., Steindler, C., Pellegrini, S., Schanen, N.C., Warren, S.T., and Geschwind, D.H. (2007). Genome-wide expression profiling of lymphoblastoid cell lines distinguishes different forms of autism and reveals shared pathways. Hum. Mol. Genet. *16*, 1682–1698.

Nowicki, S.T., Tassone, F., Ono, M.Y., Ferranti, J., Croquette, M.F., Goodlin-Jones, B., and Hagerman, R.J. (2007). The Prader-Willi phenotype of fragile X syndrome. J. Dev. Behav. Pediatr. *28*, 133–138.

Pettersen, E.F., Goddard, T.D., Huang, C.C., Couch, G.S., Greenblatt, D.M., Meng, E.C., and Ferrin, T.E. (2004). UCSF Chimera–a visualization system for exploratory research and analysis. J. Comput. Chem. *25*, 1605–1612.

Pfeiffer, B.E., and Huber, K.M. (2006). Current advances in local protein synthesis and synaptic plasticity. J. Neurosci. *26*, 7147–7150.

Pilo Boyl, P., Di Nardo, A., Mulle, C., Sassoe-Pognetto, M., Panzanelli, P., Mele, A., Kneussel, M., Costantini, V., Perlas, E., Massimi, M., et al. (2007). Profilin2 contributes to synaptic vesicle exocytosis, neuronal excitability, and novelty-seeking behavior. EMBO J. *26*, 2991–3002.

Richter, J.D., and Sonenberg, N. (2005). Regulation of cap-dependent translation by eIF4E inhibitory proteins. Nature *433*, 477–480.

Richter, J.D., and Klann, E. (2007). Translational Control of Synaptic Plasticity and Learning and Memory (Cold Spring Harbor: Cold Spring Harbor Laboratory Press), pp. 489–510.

Schaeffer, C., Bardoni, B., Mandel, J.L., Ehresmann, B., Ehresmann, C., and Moine, H. (2001). The fragile X mental retardation protein binds specifically to its mRNA via a purine quartet motif. EMBO J. *20*, 4803–4813.

Schenck, A., Bardoni, B., Moro, A., Bagni, C., and Mandel, J.L. (2001). A highly conserved protein family interacting with the fragile X mental retardation protein (FMRP) and displaying selective interactions with FMRP-related proteins FXR1P and FXR2P. Proc. Natl. Acad. Sci. USA *98*, 8844–8849.

Schenck, A., Bardoni, B., Langmann, C., Harden, N., Mandel, J.L., and Giangrande, A. (2003). CYFIP/Sra-1 controls neuronal connectivity in Drosophila and links the Rac1 GTPase pathway to the fragile X protein. Neuron *38*, 887–898.

Schratt, G.M., Nigh, E.A., Chen, W.G., Hu, L., and Greenberg, M.E. (2004). BDNF regulates the translation of a select group of mRNAs by a mammalian target of rapamycin-phosphatidylinositol 3-kinase-dependent pathway during neuronal development. J. Neurosci. *24*, 7366–7377.

Skryabin, B.V., Sukonina, V., Jordan, U., Lewejohann, L., Sachser, N., Muslimov, I., Tiedge, H., and Brosius, J. (2003). Neuronal untranslated BC1 RNA: targeted gene elimination in mice. Mol. Cell. Biol. *23*, 6435–6441.

Steward, O., and Schuman, E.M. (2003). Compartmentalized synthesis and degradation of proteins in neurons. Neuron *40*, 347–359.

Takei, N., Kawamura, M., Hara, K., Yonezawa, K., and Nawa, H. (2001). Brain-derived neurotrophic factor enhances neuronal translation by activating multiple initiation processes: Comparison with the effects of insulin. J. Biol. Chem. *276*, 42818–42825.

Tashiro, A., and Yuste, R. (2004). Regulation of dendritic spine motility and stability by Rac1 and Rho kinase: Evidence for two forms of spine motility. Mol. Cell. Neurosci. *26*, 429–440.

Tomoo, K., Matsushita, Y., Fujisaki, H., Abiko, F., Shen, X., Taniguchi, T., Miyagawa, H., Kitamura, K., Miura, K., and Ishida, T. (2005). Structural basis for mRNA Cap-Binding regulation of eukaryotic initiation factor 4E by 4E-binding protein, studied by spectroscopic, X-ray crystal structural, and molecular dynamics simulation methods. Biochim. Biophys. Acta *1753*, 191–208.

Weiler, I.J., and Greenough, W.T. (1993). Metabotropic glutamate receptors trigger postsynaptic protein synthesis. Proc. Natl. Acad. Sci. USA *90*, 7168–7171.

Weiler, I.J., Irwin, S.A., Klintsova, A.Y., Spencer, C.M., Brazelton, A.D., Miyashiro, K., Comery, T.A., Patel, B., Eberwine, J., and Greenough, W.T. (1997).

Fragile X mental retardation protein is translated near synapses in response to neurotransmitter activation. Proc. Natl. Acad. Sci. USA *94*, 5395–5400.

West, N., Roy-Engel, A.M., Imataka, H., Sonenberg, N., and Deininger, P. (2002). Shared protein components of SINE RNPs. J. Mol. Biol. *321*, 423–432.

Westmark, C.J., and Malter, J.S. (2007). FMRP mediates mGluR5-dependent translation of amyloid precursor protein. PLoS Biol. *5*, e52.

Yin, Y., Edelman, G.M., and Vanderklish, P.W. (2002). The brain-derived neurotrophic factor enhances synthesis of Arc in synaptoneurosomes. Proc. Natl. Acad. Sci. USA *99*, 2368–2373.

Zalfa, F., Giorgi, M., Primerano, B., Moro, A., Di Penta, A., Reis, S., Oostra, B., and Bagni, C. (2003). The fragile X syndrome protein FMRP associates with BC1 RNA and regulates the translation of specific mRNAs at synapses. Cell *112*, 317–327.

Zalfa, F., Adinolfi, S., Napoli, I., Kuhn-Holsken, E., Urlaub, H., Achsel, T., Pastore, A., and Bagni, C. (2005). Fragile X mental retardation protein (FMRP) binds specifically to the brain cytoplasmic RNAs BC1/BC200 via a novel RNA-binding motif. J. Biol. Chem. *280*, 33403–33410.

Zalfa, F., Eleuteri, B., Dickson, K.S., Mercaldo, V., De Rubeis, S., di Penta, A., Tabolacci, E., Chiurazzi, P., Neri, G., Grant, S.G., and Bagni, C. (2007). A new function for the fragile X mental retardation protein in regulation of PSD-95 mRNA stability. Nat. Neurosci. *10*, 578–587.

Zhang, Y.Q., Bailey, A.M., Matthies, H.J., Renden, R.B., Smith, M.A., Speese, S.D., Rubin, G.M., and Broadie, K. (2001). Drosophila fragile X-related gene regulates the MAP1B homolog Futsch to control synaptic structure and function. Cell *107*, 591–603.

Zhang, M., Wang, Q., and Huang, Y. (2007). Fragile X mental retardation protein FMRP and the RNA export factor NXF2 associate with and destabilize Nxf1 mRNA in neuronal cells. Proc. Natl. Acad. Sci. USA *104*, 10057–10062.